

Phase transition in ordered porphyrin layers on iodide modified Cu(111): An EC-STM study

N.T.M. Hai ^a, B. Gasparovic ^b, K. Wandelt ^{a,*}, P. Broekmann ^a

^a Institute of Physical and Theoretical Chemistry, Bonn University, Wegeler-Strasse 12, D-53115 Bonn, Germany

^b Center for Marine and Environmental Research, Rudjer Boskovic Institute, Bijenicka 54, 10000 Zagreb, Croatia

Available online 25 May 2007

Abstract

The self-assembly of meso-tetra (*N*-methyl-4-pyridyl) porphyrine tetratosylat (H_2TMPyP) on an iodide modified Cu(111) surface has been studied by means of in situ electrochemical-scanning tunneling microscopy (EC-STM). The I/Cu(111) surface was found to be a good substrate for the self-assembly of highly ordered layers of porphyrin cations. Furthermore, a reversible structural phase transition within the highly ordered porphyrin layer was observed during variation of the electrode potential, as a consequence of changing electronic properties of the substrate.

© 2007 Published by Elsevier B.V.

Keywords: Self-assembly; Porphyrins; Solid–liquid interface; Copper; Scanning tunneling microscopy

1. Introduction

As a “bottom-up” technique in nanotechnology, the self-assembly of atoms and molecules such as porphyrins on well-defined surfaces is getting more and more attention because it promises to create surface patterns with nanometer dimension [1], which for instance exhibit specific electronic, sensoric or catalytic functionality [2,3]. Porphyrins are biological relevant substances due to their electronic and reactive properties that can be exploited both in the biological field and in technology. Porphyrins are well-known to play a very important role in natural vital processes such as in heme for the transfer and storage of oxygen in blood, or in chlorophyll for the photosynthesis of green plants. Furthermore, they can also be used to produce drugs for the photodynamic therapy [4], as electrocatalysts for the reduction of inorganic and organic nitro compounds [5,6], or in form of assemblies as chemical sensors [7]. Especially, tetra (*N*-methyl-4-pyridyl)-porphyrin molecules (TMPyP) were proven to be sensors for the

detection of benzene and heavy metal ions (Hg^{2+} , and Pb^{2+} , Cd^{2+}) [8].

Our system of choice is the self-assembly of meso-tetra (*N*-methyl-4-pyridyl) porphyrine tetratosylat (H_2TMPyP) (Fig. 1) on an iodide modified Cu(111) surface from solution. The molecules are expected to lie flat on the bare metal surface due to their large planar π system so that the π bonding to the surface can be maximized [9]. In solution, the positively charged cations (Fig. 1) are expected to interact strongly electrostatically with negatively charged well-defined electrode surfaces, so that the latter should be ideal substrates for the adsorption of these molecules. In fact, highly ordered adlayers of H_2TMPyP were already found on typical anion modified electrode surfaces such as I/Au(111), I/Pt(100), I/Ag(111) and I/Au(111) [10–14], while studies on the self-assembly of porphyrins on more reactive copper single crystal electrodes have not yet been reported. Only under ultrahigh vacuum (UHV) conditions the adsorption of porphyrin molecules has been studied on bare copper surfaces [15,16].

In this contribution, we present and discuss results on the adsorption of H_2TMPyP on an iodide modified Cu(111) electrode as obtained by high resolution in situ

* Corresponding author. Tel.: +49 228 73 2253; fax: +49 228 73 2515.
E-mail address: k.wandelt@uni-bonn.de (K. Wandelt).

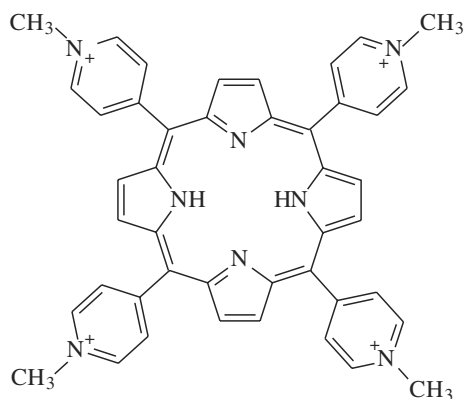


Fig. 1. Structural formula of the H_2TMPyP molecular cations.

electrochemical scanning tunneling microscopy (EC-STM). Unlike previous workers [10–13], we investigated the self-assembly process within the potential range, where this porphyrin is already reduced by the first two electron transfer step [17,18]. We found structural phase transitions within the porphyrin ordered layers driven by changes of the electrode potential.

2. Experimental

All the in situ measurements were carried out using a home-built electrochemical scanning tunneling microscope at constant current mode [19,20].

The Cu(111) electrode (MaTeck company, Juelich, Germany) was electropolished before each STM measurement in order to remove contaminations and the native copper oxide layer on the surface by dipping the electrode in 50% orthophosphoric acid at an anodic potential of 2 V for 40 s. The surface was then rinsed carefully with the degassed

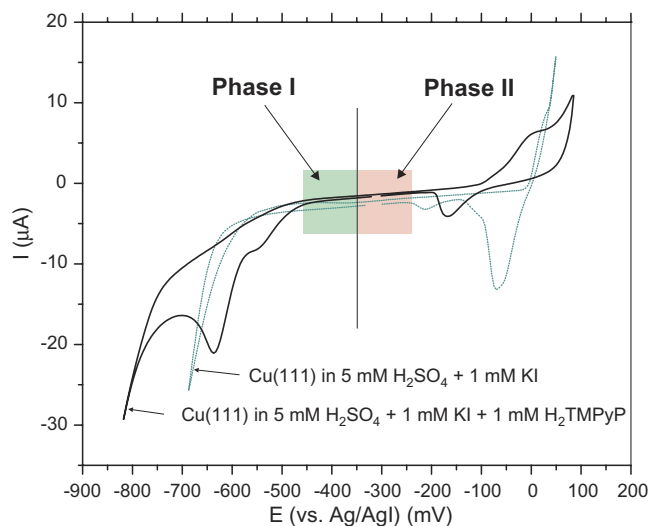


Fig. 2. Cyclic voltammograms of Cu(111) in (5 mM H_2SO_4 + 1 mM KI)- and in (5 mM H_2SO_4 + 1 mM KI + 1 mM H_2TMPyP)-solution; scan rate 10 mV/s.

supporting electrolyte used for the subsequent adsorption experiments (5 mM H_2SO_4) before mounting it into the electrochemical cell. The potential of the copper electrode was controlled with respect to an AgI/Ag reference electrode; normally a value within the potential range of the double layer regime was chosen (Fig. 2). For the adsorption experiments the supporting electrolyte in the cell was displaced by a solution containing sulfate, iodide and porphyrin (5 mM H_2SO_4 + 1 mM KI + 1 mM H_2TMPyP).

All the electrolytes used were prepared with high purity water (Milli-Q purification system, $>18 M\Omega$ cm, TOC <4 ppb) and purged with suprapure argon gas for several hours before use. The porphyrin (H_2TMPyP) (suprapure,

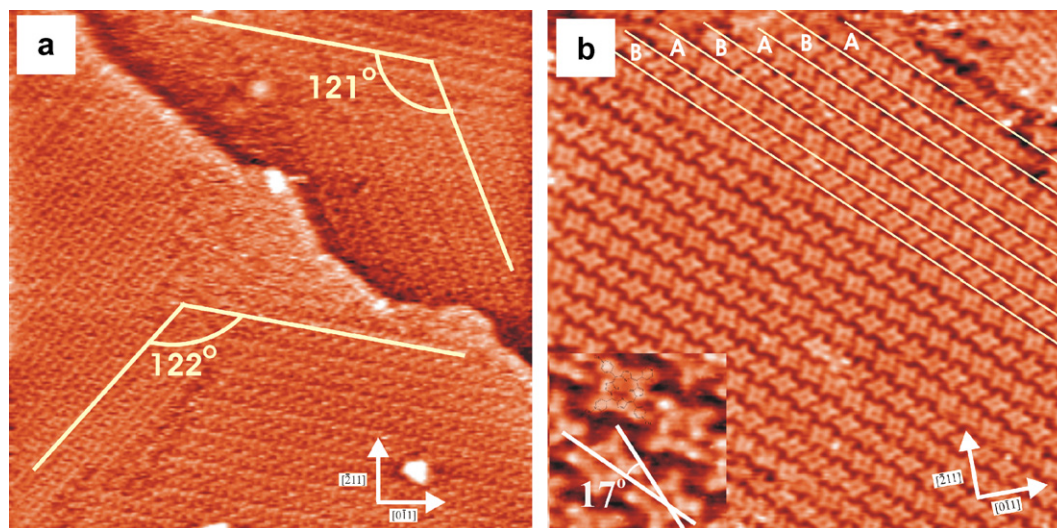


Fig. 3. STM images of an H_2TMPyP layer on iodide modified Cu(111) (phase I) (a) monolayer with three rotational domains; image parameters: $41.10 \text{ nm} \times 41.00 \text{ nm}$; $I_t = 0.1 \text{ nA}$, $U_b = 416 \text{ mV}$, $E = -350 \text{ mV vs Ag/AgI}$; (b) molecular arrangement; image parameters: $27.77 \text{ nm} \times 27.70 \text{ nm}$; $I_t = 0.1 \text{ nA}$, $U_b = 135 \text{ mV}$, $E = -350 \text{ mV vs Ag/AgI}$; inset: Molecular rotation by 17° vs direction of rows. The small arrows indicate crystallographic directions ($\bar{2}11$) and ($1\bar{1}0$) of the Cu(111)-substrate.

halide free, Scientific Frontier), potassium iodide and sulfuric acid (suprapure, Merck) were used without any further purification.

The tunneling tips were electrochemically etched from a 0.25 mm diameter tungsten wire in 2 M KOH electrolyte, rinsed with high purity water, dried, and isolated by passing them through a drop of hot glue.

3. Results and discussion

For illustration, Fig. 2 shows the cyclic voltammograms (CVs) of the Cu(111) electrode in (5 mM H₂SO₄ + 1 mM KI)- as well as in (5 mM H₂SO₄ + 1 mM KI + 1 mM H₂TMPyP)-solution. The structural investigations presented here are exclusively carried out within the central potential regime between -250 mV and -450 mV. The prominent structures in both CVs at more positive potentials, i.e. the copper dissolution and redeposition and also

the formation and dissolution of 2D-CuI compound [21,22], and at more negative potentials, i.e. the redox-behavior of the porphyrins and the retardation of the hydrogen evolution reaction (HER) will be discussed in greater detail in a forthcoming paper [18]. Here, we place emphasis on the observed adlayer structures and their transitions purely driven by changes of the electrode potential and not by redox-modifications of the adsorbed species. It is well known that iodide anions adsorb specifically on the Cu(111) surface and form highly ordered layers, whose structure is potential dependent in terms of electro-compression or -expansion [23]. However, within the potential range examined here, iodide forms a commensurate ($\sqrt{3} \times \sqrt{3}$)R30° structure on Cu(111) with three fold symmetry [23].

Fig. 3 shows a highly ordered layer of H₂TMPyP on the thus iodide modified Cu(111) surface at an electrode potential of -350 mV vs. Ag/AgI. The surface is covered

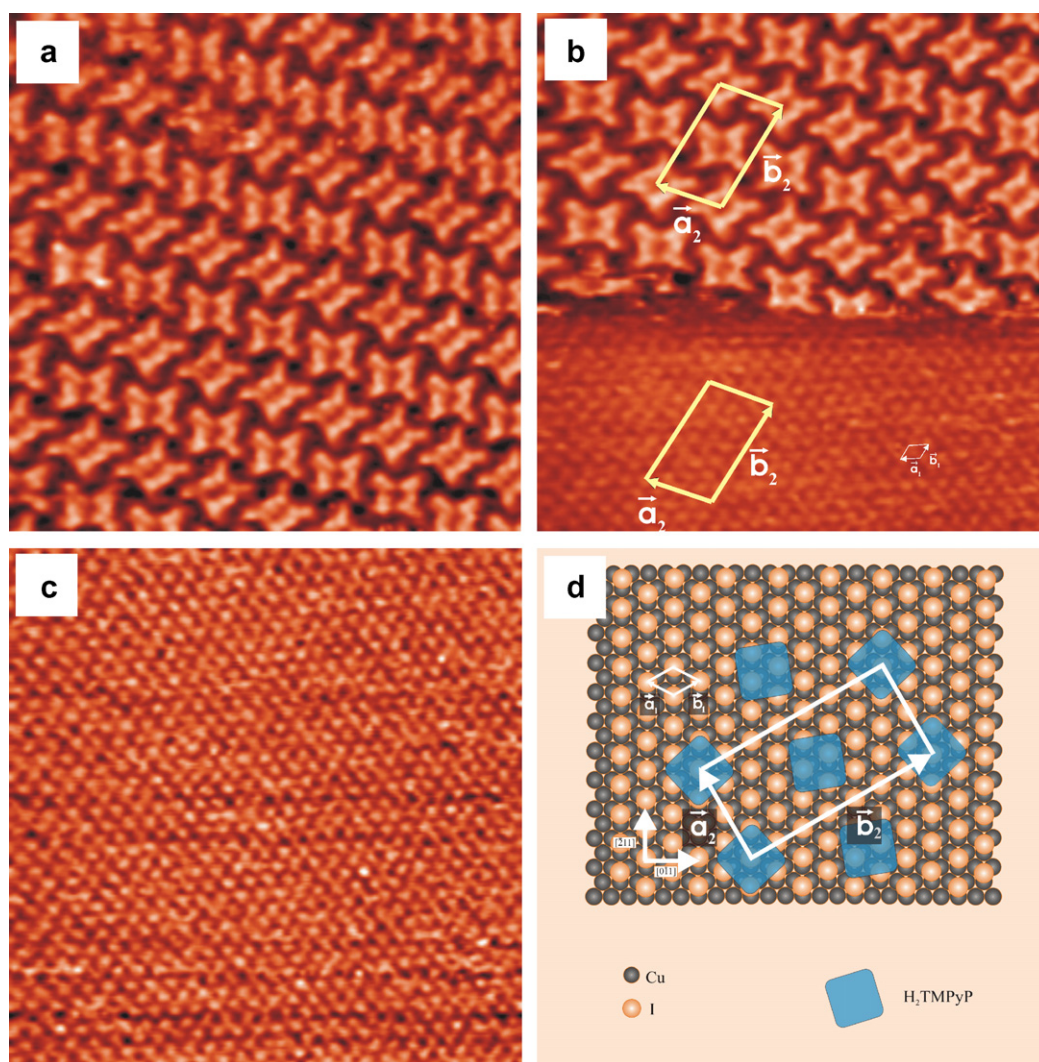


Fig. 4. Structural correlation between the H₂TMPyP layer and the underlying iodide lattice (see text); image parameters: (a) 12.20 nm × 12.17 nm; $I_t = 0.25$ nA, $U_b = 211$ mV, $E = -380$ mV vs Ag/AgI; (b) 12.20 nm × 12.17 nm; $I_t = 0.25$ –0.5 nA, $U_b = 211$ –18 mV, $E = -380$ mV vs Ag/AgI; (c) 12.20 nm × 12.17 nm; $I_t = 0.5$ nA, $U_b = 18$ mV, $E = -380$ mV vs Ag/AgI; (d) structure model of H₂TMPyP on Cu(111)/I; ($\bar{2}11$) and ($0\bar{1}1$) refer to crystallographic directions of the Cu substrate; (\bar{a}_1, \bar{b}_1) indicate the iodide unit cell, and (\bar{a}_2, \bar{b}_2) that of the porphyrin layer.

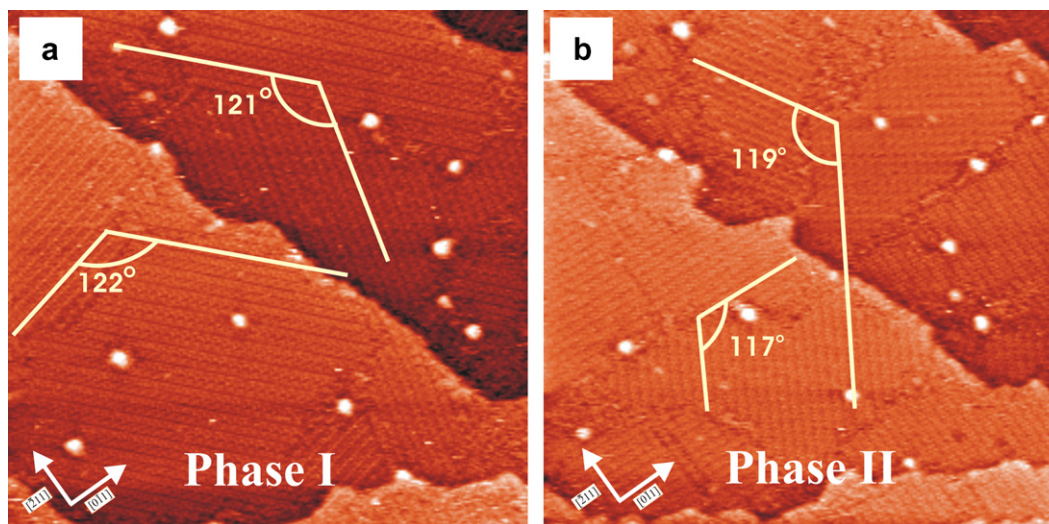


Fig. 5. Potential induced phase transition from phase I to phase II; image parameters: (a) 68.50 nm \times 68.33 nm; $I_t = 0.1$ nA, $U_b = 421$ mV, $E = -400$ mV vs Ag/AgI; (b) 68.50 nm \times 68.33 nm; $I_t = 0.1$ nA, $U_b = 358$ mV $E = -300$ mV vs Ag/AgI; (211) and (110) indicate crystallographic directions of the Cu substrate.

almost entirely by porphyrin molecules. Three domains, which are rotated by 120° with respect to each other are seen in Fig. 3a. (The slight deviation from the perfect value of 120° is ascribed to drift during imaging).

The molecular arrangement within each domain of the porphyrin layer can be seen more clearly in Fig. 3b. The molecules are ordered in rows. All molecules within one row are rotated with respect to the direction of the row by either $+17^\circ$ or -17° (see inset in Fig. 3b). The shape of the individual molecules agrees with their quadric structure (Fig. 1) which, in turn, indicates that the molecules lie flat on the surface. The existence of just three rotational domains (Fig. 3a) suggests a tight structural relationship between the porphyrin layer and the iodide covered Cu(111) surface underneath.

In order to acquire more detailed information about the structural correlation between the porphyrin layer and the substrate the series of STM images of 12.20 nm \times 12.20 nm shown in Fig. 4a–c was recorded successively at the same surface area. At moderate tunneling conditions, i.e. at lower tunneling current I_t , at which the tunneling tip is further away from the surface, the porphyrin layer is displayed with high sub-molecular resolution (Fig. 4a). By increasing I_t during scanning, the tip comes closer to the surface. As a consequence, the porphyrin molecules are swept away, and the iodide layer underneath becomes clearly visible (Fig. 4b and c). This experiment, in particular Fig. 4b, enables a direct correlation between the structure of the organic overlayer and that of the underlying iodide lattice. As a result, the molecular rows run evidently parallel to the $\langle 110 \rangle$ direction of the iodide layer or, correspondingly, parallel to the close-packed atom rows of the Cu(111) surface. One unit cell of the adlayer with two porphyrin molecules as shown in Fig. 4b (\vec{a}_2, \vec{b}_2) with $a_2 = 6a_{\text{Cu}} = 1.536$ nm and $b_2 = 7\sqrt{3}a_{\text{Cu}} = 3.104$ nm can

be described by a matrix $\begin{pmatrix} 4 & -2 \\ 0 & 7 \end{pmatrix}$ with respect to the iodide lattice. A structure model of the porphyrin lattice on I/Cu(111) is presented in Fig. 4d. As a result of substrate symmetry, three domains of this ordered porphyrin structure are expected, in agreement with the experimental observation displayed in Fig. 3a. The porphyrin surface coverage was calculated to be 0.0714 ML relative to the iodide underlayer, or 4.2×10^{13} molecules/cm 2 .

One advantage of the electrochemical over the UHV environment is, that simple variations of the electrode potential may lead to controlled changes of the surface properties. In the present context we have therefore, recorded a series of ECSTM images, each taken after changing the electrode potential in anodic direction. Fig. 5 shows two images from this series obtained at -400 mV and -300 mV vs. Ag/AgI, respectively. Both images truly cover the same surface area as verified by the bright dots as markers arising from surface defects. Even though the porphyrin forms highly ordered monolayers with rows of molecules and at least three rotational domains (120°) at both potential values, the direction of the molecular rows is completely different at both potentials. Obviously, a structural phase transition has occurred from phase I at -400 mV to a new phase at -300 mV (phase II). Since the porphyrin molecules themselves do not undergo any further redox-modification within this potential range (Fig. 2) the observed phase transition must be a consequence of altered molecule-substrate interactions.

Structural details of the porphyrin phase II and its correlation with the iodide lattice underneath can again be gained from high resolution images as shown in Fig. 6. Within each domain of phase II all molecules have the same relative orientation and form (after drift correction) an almost quadratic lattice (Fig. 6a). In contrast to phase I, however, molecular rows of phase II do not follow any

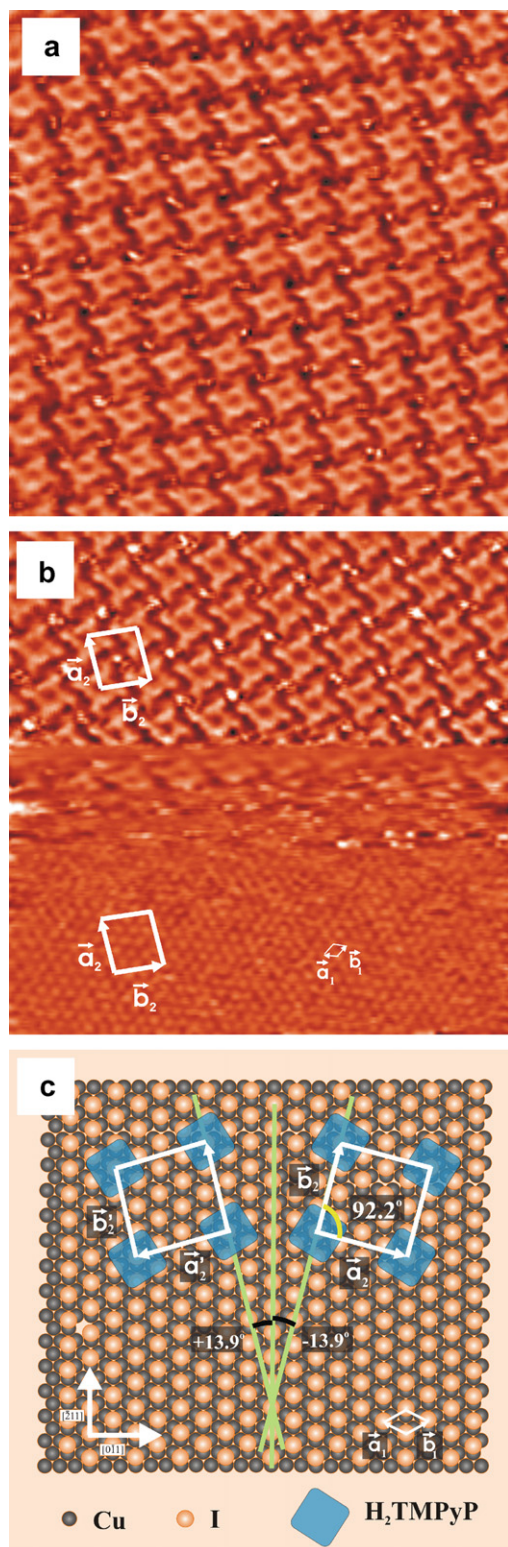


Fig. 6. STM images of an H_2TMPyP layer on iodide modified Cu(111) (phase II), image parameters: (a) $13.88 \text{ nm} \times 13.85 \text{ nm}$; $I_t = 0.14 \text{ nA}$, $U_b = 136 \text{ mV}$, $E = -250 \text{ mV}$ vs Ag/AgI; (b) $13.88 \text{ nm} \times 13.85 \text{ nm}$; $I_t = 0.1\text{--}5 \text{ nA}$, $U_b = 136\text{--}46 \text{ mV}$, $E = -250 \text{ mV}$ vs Ag/AgI; (c) structure model of H_2TMPyP on I/Cu(111)–phase II – with two mirror domains within one of three rotational domains; $(\bar{2}11)$ and $(0\bar{1}1)$ indicate crystallographic directions of the Cu substrate, (\vec{a}_1, \vec{b}_1) indicate the unit cell of the iodide layer, (\vec{a}_2, \vec{b}_2) and (\vec{a}'_2, \vec{b}'_2) span the unit cell of the porphyrin overlayer.

high symmetry direction of the substrate, neither of the iodide lattice nor of the Cu(111) surface. The unit cell of phase II ($a_2 = b_2 = 1.5897 \text{ nm}$, $\alpha = 92.2^\circ$) as depicted in Fig. 6b contains one porphyrin molecule and can be related to the iodide lattice by the matrix $\begin{pmatrix} 4 & 1 \\ 1 & 4 \end{pmatrix}$.

A structure model of phase II (\vec{a}_2, \vec{b}_2) is presented in Fig. 6c. By symmetry of the lattice, a mirror structure (\vec{a}'_2, \vec{b}'_2) with respect to a close-packed iodide row must exist which together with the three rotational domains (Fig. 5b) results in the coexistence of a total of six domains. (Considering the orientation of the individual molecules the symmetry is further reduced and, actually, results in a total of twelve domains.) The surface coverage per domain of phase II was calculated to be 0.0667 ML with respect to the iodide lattice underneath, or 3.92×10^{13} molecules/cm², that is slightly diluted compared to phase I.

In summary, the transition from phase I at -400 mV to phase II at -300 mV manifests itself by (a) an obvious structural rearrangement of the porphyrin molecules and (b) a change in surface coverage. While in phase I the molecular rows of each domain are parallel to high symmetry directions of the I/Cu(111) substrate, this is not the case for phase II. This suggests a stronger porphyrin-substrate interaction in phase I than in phase II. The reduced molecular density, i.e. the lower coverage, of phase II compared to phase I points in the same direction.

In general, the formation of ordered layers as those observed here from porphyrin molecules on the $(\sqrt{3} \times \sqrt{3})R30^\circ$ I/Cu(111) surface is the result of a sensitive equilibrium between adsorbate–adsorbate and adsorbate–substrate interactions. A change of either one or both will be the reason of a structural transition. In the present case, within the relatively narrow potential window of -400 mV – -300 mV the porphyrin molecules exhibit no further redox activity; their lateral interaction should therefore basically remain unaltered. Likewise, the iodide underlayer retains, within the accuracy of the experiment, its $\sqrt{3}$ –structure, and, hence, its particle density. Consequently, a driving force for the observed structural transition from phase I at -400 mV to phase II at (the more positive potential of) -300 mV arises from the decrease of negative charge density within the I/Cu(111) substrate surface, and, hence, a reduced electrostatic interaction between the porphyrin cations and the substrate underneath. This reduced electrostatic attraction holds somewhat less porphyrin cations at the surface, i.e. the coverage decreases. The (repulsive) interactions between the porphyrin cations within the adlayer are responsible for their lateral arrangement. In total, however, the adsorbate–adsorbate- and adsorbate–substrate-interactions are such that the molecular cations are still mobile enough to reach their equilibrium positions and orientations, and to form an ordered layer. This is consistent with the fact that the observed phase transition was found to be reversible.

4. Summary

Highly ordered H₂TMPyP-layers on an iodide modified Cu(111) electrode surface have been observed and characterized by means of in situ electrochemical scanning tunneling microscopy (EC-STM). Besides the van der Waals force between the porphyrin and the iodide modified copper substrate the electrostatic forces between them are believed to play an important role in the formation of porphyrin ordered layer and the potential dependence phase transition. A change of these electrostatic forces by changing the electrode potential from –400 mV to –300 mV is also taken responsible for the observed structural transition from a phase I to a slightly less dense phase II with different molecular orientation. This explanation is supported by the fact that the two-dimensional porphyrin lattice of phase I coincides with high symmetry directions of the I/Cu(111) substrate, while this is not the case with phase II. The results offer the possibility to create different self-assembled organic layers on a suitably modified metal surface from solution by controlling the electrochemical potential of the electrode.

Acknowledgements

This work was funded by the German Academic Exchange Service (DAAD) and the SFB 624 of the German Science Foundation.

References

- [1] J.V. Barth, G. Costantini, K. Kern, *Nature* 437 (2005) 671.
- [2] G.S. Kottas, L.I. Clarke, D. Horinek, J. Michl, *Chemical Reviews* 105 (2005) 1281.
- [3] D.M. Vriezema, M.C. Aragoes, J. Elemans, J. Cornelissen, A.E. Rowan, R.J.M. Nolte, *Chemical Reviews* 105 (2005) 1445.
- [4] S.P.S. Tita, J.R. Perussi, *Brazilian Journal of Medical and Biological Research* 34 (2001) 1331.
- [5] J. Lei, H. Ju, O. Ikeda, *Electrochimica Acta* 49 (2004) 2453.
- [6] S.-M. Chen, S.-V. Chen, *Electrochimica Acta* 48 (2003) 4049.
- [7] R. Purrello, S. Gurrieri, R. Lauceri, *Coordination Chemistry Reviews* 192 (1999) 683.
- [8] D. Delmarre, R. Meallet, C. Bied-Charreton, R.B. Pansu, *Journal of Photochemistry and Photobiology A-Chemistry* 124 (1999) 23.
- [9] Y. He, T. Ye, E. Borguet, *Journal of the American Chemical Society* 124 (2002) 11964.
- [10] M. Kunitake, N. Batina, K. Itaya, *Langmuir* 11 (1995) 2337.
- [11] M. Kunitake, U. Akiba, N. Batina, K. Itaya, *Langmuir* 13 (1997) 1607.
- [12] K. Ogaki, N. Batina, M. Kunitake, K. Itaya, *Journal of Physical Chemistry* 100 (1996) 7185.
- [13] K. Sashikata, T. Sugata, M. Sugimasa, K. Itaya, *Langmuir* 14 (1998) 2896.
- [14] L.J. Wan, S. Shundo, J. Inukai, K. Itaya, *Langmuir* 16 (2000) 2164.
- [15] X.L. Guo, Z.C. Dong, A.S. Trifonov, K. Miki, K. Kimura, S. Mashiko, *Applied Surface Science* 241 (2005) 28.
- [16] X.L. Guo, Z.C. Dong, A.S. Trifonov, K. Miki, K. Kimura, S. Mashiko, *Applied Physics A-Materials Science & Processing* 81 (2005) 367.
- [17] B.P. Neri, G.S. Wilson, *Analytical Chemistry* 44 (1972) 1002.
- [18] N.T.M. Hai, K. Wandelt, P. Broekmann, in preparation.
- [19] M. Wilms, PhD Thesis, Bonn, 1999.
- [20] M. Wilms, M. Kruff, G. Bermes, K. Wandelt, *Review of Scientific Instruments* 70 (1999) 3641.
- [21] P. Broekmann, N.T.M. Hai, H.K. Wandelt, *Surface Science* 600 (2006) 3971.
- [22] P. Broekmann, N.T.M. Hai, K. Wandelt, *Journal of Applied Electrochemistry* 36 (2006) 1241.
- [23] B. Obliers, P. Broekmann, K. Wandelt, *Journal of Electroanalytical Chemistry* 554 (2003) 183.